Pergamon

Cement and Concrete Research 32 (2002) 1907–1914

CEMENT AND CONCRETE RESEARCH

Evolution of the capillary network in a reactive powder concrete during hydration process

V. Morin[a,*], F. Cohen-Tenoudji[a], A. Feylessoufi[b], P. Richard[c]

[a]*Laboratoire Universitaire d'Application de la Physique (LUAP), Université Paris VII, 2, Place Jussieu, 75005 Paris, France*
[b]*Centre de Recherche sur la Matière Divisée (CRMD), CNRS and Université d'Orléans, 45071 Orléans Cedex, France*
[c]*Département de Génie Civil, Université de Sherbrooke, Sherbrooke, Quebec, Canada J1K2R1*

Received 20 October 1999; accepted 4 June 2002

Abstract

Ultrasonic waves in echographic mode, combined with autogenous shrinkage measurements, were used to study the evolution of the capillary network of reactive powder concrete (RPC) from the time after the mixing. Two characteristic porous classes have been identified: the first, between 10 and 20 nm, begins when the material reaches its solid hyperstatic state, and the second about 1 or 2 nm. The first class is associated with the porous space between the C-S-H hydrate clusters and the second with the internal porosity of the hydrate. The evolution of the active capillary radius as a function of the degree of hydration allows us to understand the strong interaction between the capillary network size and the chemical activity given by the dissipated calorimetric power curve. Indeed, the maximum point of the chemical activity marks the transition of the first class of pores to the second one. Finally, measurements of electrical conductivity through RPC samples show that after the maximum of the dissipated power, the curve of this electrical conductivity presents the same evolution as the capillary radius. As the electrical conductivity clearly depends on the evolution of the capillary network, the similarity between the results confirms our analysis in pore classes.

Keywords: Concrete; Ultrasonic spectroscopy; Shrinkage; Capillary network; Electrical conductivity

1. Introduction

High-performance concretes, and more precisely, reactive powder concretes (RPCs) have been elaborated by the improvement of several parameters such as particle-size homogeneity, porosity and microstructure. Compressive strengths ranging between 200 and 800 MPa, fracture energies between 1200 and 40000 J/m^2 and ultimate tensile strain before fracture of the order of 1% are reached [1].

The study of the capillary network of these new concretes has been achieved by the use of both ultrasonic and autogenous shrinkage measurements. In the case of the ultrasonic technique, instead of using transmission measurements [2,3], we have developed an echographic method [4,5]. Contrary to the transmission measurements, with this technique we can acquire ultrasonic signals in both longitudinal and shear waves since the mixing. Moreover, the frequency range used is not limited to the very low frequencies that are normally well adapted to the transmission measurements due to the high acoustic absorption of the paste after mixing. This large frequency range used in this study allows the analysis of the material under different scales. Finally, in the echographic technique, the ultrasonic waves interact only with a very small layer of the medium when reflected. As a result, the signals are not affected by the multiple scatterings of the wave by the solid particles as in the transmission technique.

In parallel with these echographic studies, we perform autogenous shrinkage measurements. This method allows us to follow the relative volumetric contraction of the specimen (taking a positive value in this paper) during the hydration processes. The two principal reasons for this volumetric contraction are the formation of hydrates, particularly C-S-H hydrates during the setting of the medium, and the presence

* Corresponding author. LAFARGE Laboratoire Central de Recherche, 95 Rue du Montmurier/BP 15, 38291 Saint Quentin Fallavier Cedex, France. Tel.: +33-4-74-82-18-24; fax: +33-4-74-95-56-23.
E-mail address: vincent.morin@pole-technologique.lafarge.com (V. Morin).

0008-8846/02/$ – see front matter © 2002 Elsevier Science Ltd. All rights reserved.
PII: S0008-8846(02)00893-1

of capillary phenomena. Indeed, the water introduced initially at mixing reacts with the anhydrous cement particles to form hydrates with a specific volume smaller than the total volume of the initial products. Moreover, in the present case of an autogenous experiment, there is no water exchange between the concrete and outside. As a result, the hydration reactions induce self-desiccation of the medium and decrease the capillary spaces which become narrower. This method is sensitive both to the building of the solid structure inside the medium and to the evolution of the capillary network.

2. Experimental

2.1. Material

The RPC used has the following components, particle size, proportion, expressed in component to cement mass ratios (in parenthesis), respectively: Type V Portland cement, 20 μm average diameter size and dry density of 3.17 (1); fine quartz sand, 310 μm average diameter and dry density of 2.65 (1.1); silica fume, 0.2 μm average diameter and dry density of 2.27 (0.25); water (0.21) and superplasticizer dry extract (0.015). This superplasticizer is a copolymer of acrylic acid with acrylic ester in water solution; it belongs to the last generation of macromolecules acting with a dual action: (i) an anionic effect brought by a negative carboxylic (COO^-) group, (ii) a volumetric steric effect given by the neutral oxyethylic branches.

For the sample preparation, the dry powders (sand, silica fume and cement) are mixed during 3 or 5 min. The water and half volume of superplasticizer are added to these dry components. This introduction of water determines the time origin of the experiment. Then, after 3 min, the second half of the volume of the superplasticizer is added, and the whole is mixed during 5 min. Finally, the mixture is degassed during 5 min using a conventional water–air pump and divided into three different samples for shrinkage, acoustic and calorimetric experiments.

2.2. Ultrasonic set-up

The ultrasonic set-up has been detailed in Ref. [5]. The concrete samples are enclosed in an ultrasonic Plexiglas cell. A pair of 1-in., 0.5-MHz transducers (one for compressional waves, the other for shear waves) is fixed on one 2-cm thick, cell wall. The cell is placed in a thermoregulated bath at 20 °C. Thermocouples are placed in the bath and in the concrete cell. Echographic signals generated by the Plexiglas–concrete interface are recorded every 5 min for the two kinds of waves for 3 days.

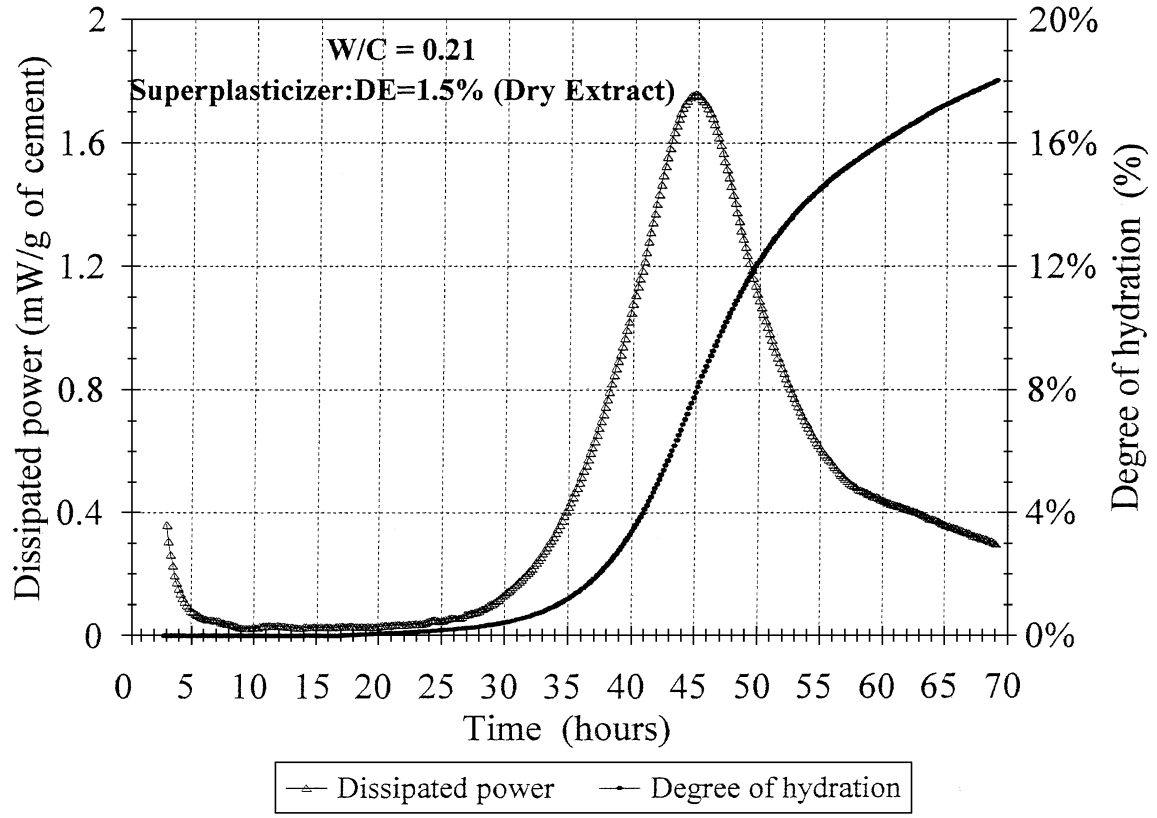

Fig. 1. Dissipated power and degree of hydration of the RPC sample as a function of time.

The ultrasonic apparatus used is an emitter–receiver built at the University Paris VII laboratory. This system can work either in transmission or in echographic mode and makes use of 16 reception and emission channels. This ultrasonic apparatus is completely computer controlled. The sonic excitation amplitude, the waveshape, and the reception and emission gains can be determined. In the different experiments, broadband transducers in longitudinal and shear waves are used. All the ultrasonic signals are digitized with a sampling frequency of 64 MHz. With a specific software called *VCOSCI*, we are able to schedule and control the experiments up to several days. This software allows the use of different thermocouples (up to nine channels) that record the thermal activity of the concrete samples.

2.3. Calorimetric monitoring and hydration degree parameter determination

Calorimetric measurements were performed in order to evaluate the degree of hydration of the RPC specimen. For this, the ultrasonic testing cell is filled with the concrete paste and a thermocouple is put in contact with the sample. Then, the whole specimen is immersed in the thermoregulated bath at 20 °C with a precision of ±0.02 °C. A second thermocouple, placed into this bath, determines the temperature difference, ΔT, between the sample and the bath, which is normally limited to 1 or 2 °C. Because of this weak temperature difference, this calorimetric method is called "isothermal calorimetry." Finally, this temperature difference is used for the evaluation of the dissipated power of the sample during the hydration process.

This dissipated power P that describes the chemical activity of the paste, is expressed by the following formula (Eq. (1)):

$$P = H\frac{\mathrm{d}(\Delta T)}{\mathrm{d}t} + \sigma\Delta T \qquad (\mathrm{mW/g\ of\ cement}) \tag{1}$$

with: H = the caloric capacity; σ = the thermal conductance.

These values of the caloric capacity and thermal conductance are obtained from two calibration measurements.

The time integration of the dissipated power P allows the calculation of the released heat Q. With this released heat, the evolution of α, the degree of hydration of the sample as a function of time, can now be evaluated. This degree α is given by the expression:

$$\alpha = \frac{Q}{Q_\infty}$$

The value of Q_∞, which determines the released heat in the case of a total hydration of cement particles, is calculated as the average of each phase enthalpy hydration

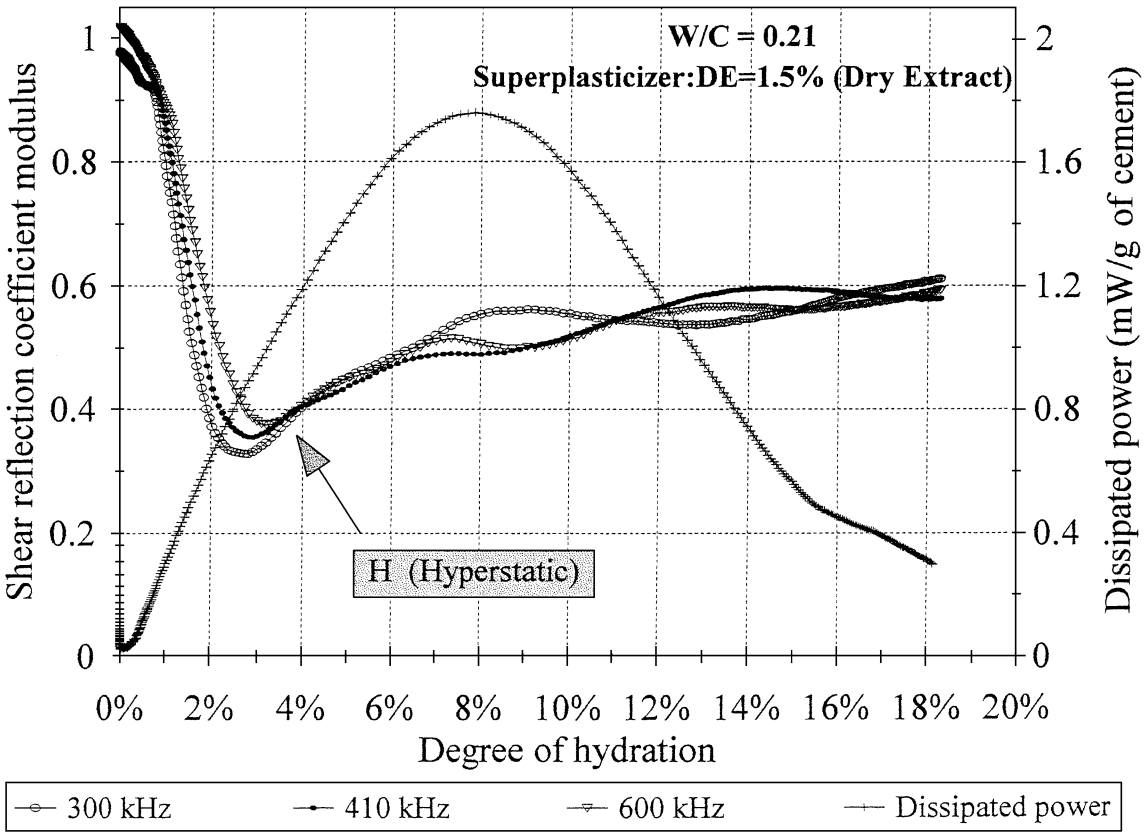

Fig. 2. Shear reflection coefficient modulus and dissipated power as a function of the degree of hydration.

reaction when taking in account the different mineralogical proportions of the anhydrous cement (weighted average). For the used cement formulation, Q_∞ is evaluated to be 483 J/g of cement.

The evolutions of the dissipated power and the degree of hydration α, after mixing and up to 70 h, for the RPC formulation used in this study, are represented in Fig. 1.

2.4. Autogenous shrinkage experiments

The shrinkage experiments were performed with a sealed sample without water exchange between the concrete paste and the external water in the regulated bath. The volumetric deformation $(\Delta V)/V$ is then named as the autogenous shrinkage. After mixing, the fresh concrete paste is poured into a thin latex container and the whole specimen is hung from a hook under a scale and is immersed in a bath thermoregulated at 20 °C. The flexibility of the latex membrane allows this container to follow the volume variations of the RPC paste during the hydration process. The weight is measured every minute. The volumetric deformation $(\Delta V)/V$ is calculated from the weight variation. The relatively high measurement rate (1 min) allows a redundancy of data used to decrease the uncertainty in the weight measurement.

3. Results and discussion

The evolutions of the shear wave reflection coefficient modulus and the dissipated power as a function of hydration degree are given in Fig. 2, which is a representation of the evolution of the solid frame rigidity during hydration. After 0.5% of hydration degree, the shear reflection coefficient modulus is strongly dependent upon the frequency. This dispersive effect stops completely between 3% and 4% of hydration degree. This determines the hyperstatic mechanical point of this RPC formulation [6]: at this stage, all the particles are linked together and the material is totally connected. However, the degree of connectivity of very small particles like silica fume remains weaker than that of the sand. The dissipated power reaches a maximum at 8% of hydration degree.

Simultaneously with echographic studies, measurements of autogenous shrinkage are made. The evolution of the relative volumetric variation $(\Delta V)/V$ and of its time derivative is represented in Fig. 3. In a previous paper [6], the evolution of this autogenous shrinkage showed a high sensitivity of the solid building mechanisms of the RPC and the development of capillary forces that are activated by the consumption of free water during the hydration process. These capillary forces induce a restart of the shrinkage,

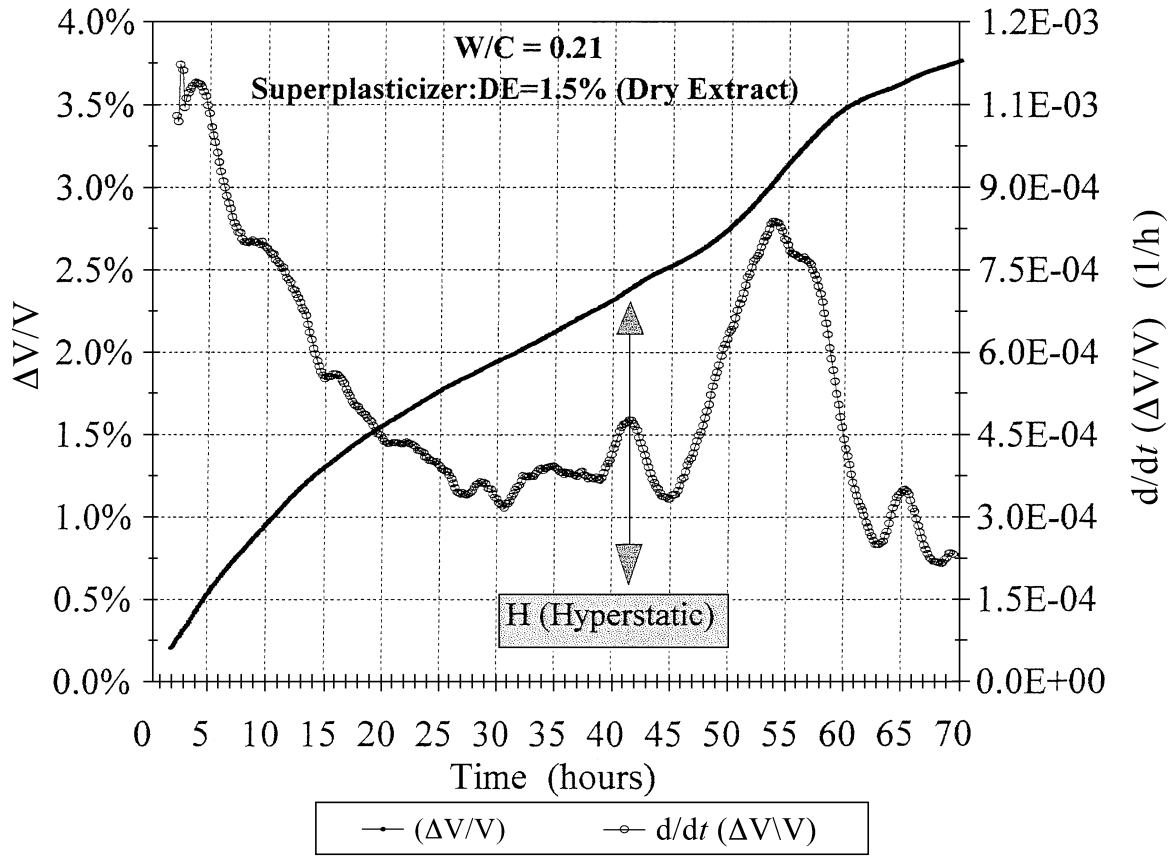

Fig. 3. Relative volumetric variation and its time derivative as a function of time.

which occurs at hour 39 and corresponds to the hyperstatic point near 3% of the degree of hydration. Also, these shrinkage measurements give some crucial information in the first hours after mixing. In these first hours, called the dormant period, an important shrinkage rate due to the balance of two different forces is noticed: capillary forces induced by the existence of air entrained between the liquid and solid phase, and repulsive electrostatic effects due to the electrical double layer formed by the solid particles surface ions and free ions of the solution around them [7]. The decrease of the repulsive electrostatic forces with the simultaneous increase in concentration of calcium ions enables the capillary force to provoke a compression of the paste at an early age. This compressive effect induces a continuous short-range granular reorganization with a stronger interaction between solid particles. So, in our measurements, we suppress the contribution of the solid particle settlement in the shrinkage in order to keep only the effects of the hydration process and of the capillary forces. The evolution of this shrinkage is given in Fig. 4 as a function of hydration degree. The inflection point of the shrinkage occurs at $\alpha = 8\%$, which corresponds to the maximum of the dissipated power. This hydration degree marks the restart of the shrinkage.

The sensitivity of our measurements leads to evaluate the evolution of the capillary network size during hydration. This mode of evaluation of the capillary pore size represents a new method to study the capillary network. It is based upon three aspects:

- The shrinkage is a slow deformation of the paste which can be attributed to a creep of the material induced by the development of internal capillary pressure. In order to evaluate the evolution of the capillary pressure, the evolution of the elastic contribution of the shrinkage has to be known. Generally, the creep is estimated to be three times higher than the elastic volumetric deformation during our experimental period [8,9].
- The capillary pressure (Δp) inside the paste is defined to be equal to the product of an elastic modulus and the elastic volumetric deformation of the paste.

$$|\Delta p| = M\frac{\Delta V}{V_{\text{elastic}}} = \frac{2\sigma}{r} \tag{2}$$

with M = elastic modulus, σ = surface tension of water at the water–air interface. In this paper, we use a value of σ independent of the pore radius ($\sigma = 73 \times 10^{-3}$ J/m^2). However, this may be questioned in the case of small capillary radius ($r < 3$ nm) [10], r = mean radius of the menisci.

- Normally, the elastic modulus used in the previous relation is the bulk modulus K. However, in the case of RPC, it was found in a previous study [6] that before the hyperstatic point, the bulk modulus is higher than the

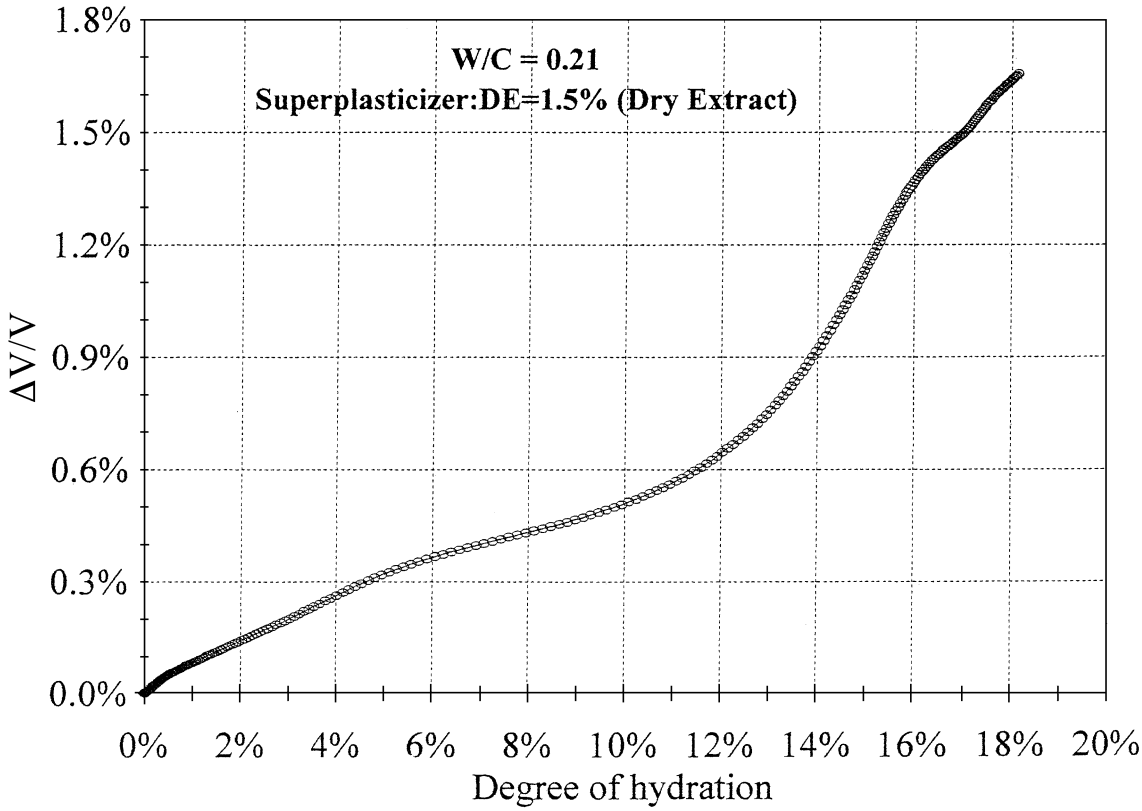

Fig. 4. Relative volumetric variation as a function of the degree of hydration.

Young's modulus E. Thus, at early ages, the modulus that must be taken into account is the Young's modulus because it represents the lower modulus of the paste. This lower modulus is the only one that can release the internal stresses imposed by the capillary pressure. After the hyperstatic point ($\alpha = 3\%$), the Young's modulus becomes higher than the bulk one and, from this point, only the bulk modulus in relation (2) is used. Then, the active elastic modulus determination follows the relation (Eq. (3)):

$$M = \text{Minimum of } (K, E) \tag{3}$$

Using these different conditions, the evolution of the mean active capillary pore radius can be calculated. We name active the part of the capillary pore network that participates in the shrinkage. Moreover, the major contribution to this shrinkage is due to the smallest pore size, which represents the strongest capillary force.

Classically, measurements of pore size are carried out on hardened specimen with higher degrees of hydration. In the technique presented in this paper, at every stage of the concrete paste maturation, the capillary network state is evaluated and its evolution analysed.

The evolutions of the active capillary radius and of the dissipated power as a function of the degree of hydration are presented in Fig. 5. At first, an important decrease of the active capillary radius in the first period between 0 and 3% of hydration degree, which leads to the hyperstatic point, is noticed. At this mechanical state, the capillary radius reaches 20 nm and the decrease of the capillary radius slows down. This slowing down continues up to $\alpha = 8\%$, which determines the maximum of the dissipated power: at this point, the active capillary radius reaches 10 nm. Then, the decrease of the dissipated power and therefore of the chemical activity is associated with a restart and a decrease of the capillary radius that is nearly equal to 2 nm at $\alpha = 15\%$. It can be supposed that after this hydration degree the evolution of the capillary radius is going to slow down because the chemical activity becomes weaker. After $\alpha = 15\%$, the active capillary radius remains nearly constant at 1–2 nm.

Between $\alpha = 3\%$ and 8%, the active capillary radius evolution slows down. In this period, the capillary radius decreases only from 20 to 10 nm. For that reason, it is supposed that these radii must represent a characteristic size of the capillary pores in the RPC. With mercury intrusion tests on hardened specimens, Baroghel-Bouny [11] has shown that the curves of pore size distribution present a maximum between 10 and 20 nm, which seems to be independent on the initial water content. This characteristic radii range represents the residual space located between the

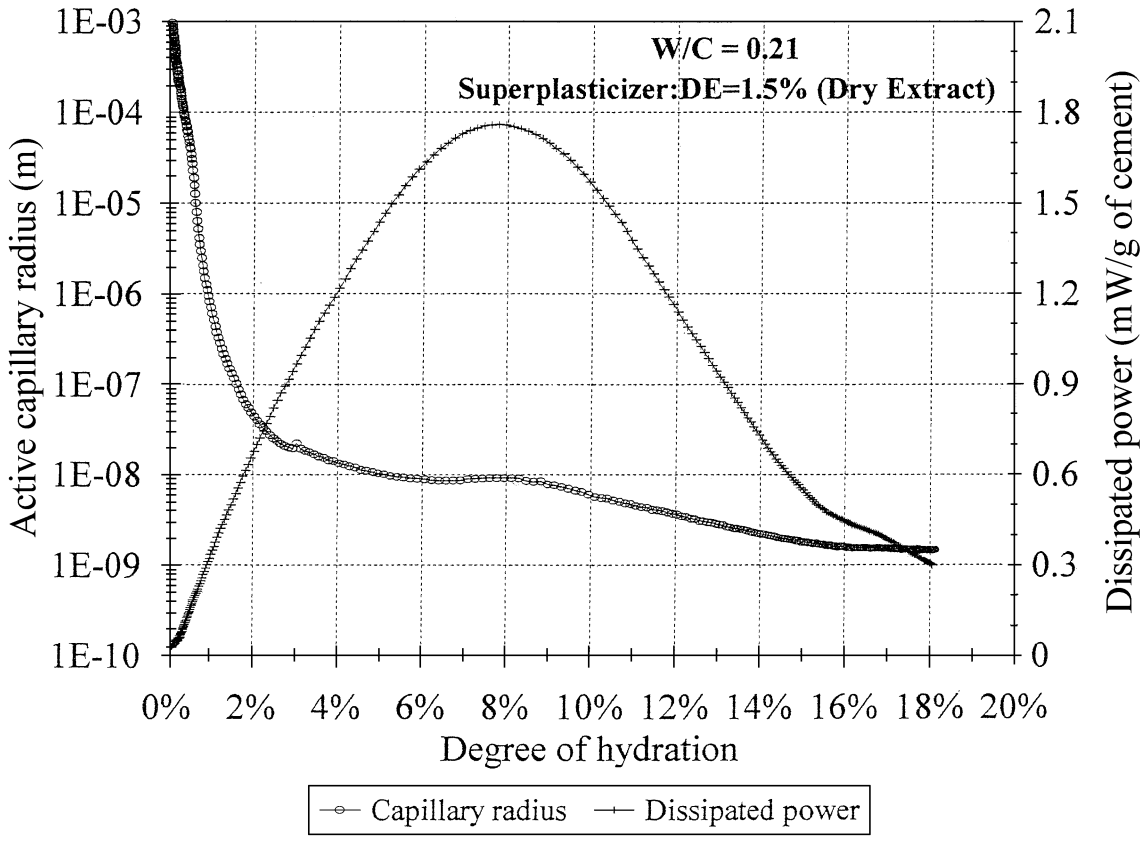

Fig. 5. Active capillary radius and dissipated power as a function of the degree of hydration.

C-S-H hydrates clusters. These results are consistent with Baroghel-Bouny's experiments. Therefore, it is noticed that these radii are activated only up to the maximum of the chemical activity.

After this maximum of the chemical activity, the active capillary radius decreases and settles down again in a second stage that can be clearly identified in Fig. 5 at $\alpha = 15\%$. At this point, the capillary radius reaches 1 or 2 nm. This stabilization of the curve determines, in a same way, a second characteristic porosity of the sample. Baroghel-Bouny observed a second maximum in the curve of pore size distribution using desorption tests near 18 Å. Thus, our experiment allows us to detect the activation time of this pore class that is attributed to the C-S-H hydrates internal porosity.

Thus, two characteristic classes of porosity have been obtained by the use of the model. The first class between 10 and 20 nm is reached at the end of the first hydration phase: up to 10 nm of pore size, the consumption of water allows the production of intergranular hydrates (outer products) that fill progressively the porous space occupied initially by the water. When the pore radii are smaller than 10 nm, a new hydration phase begins: the water is now consumed in the hydrates porosity in order to produce internal hydrates that expand by reaching the bulk of anhydrous cement particles.

Using the previous discussion, the evolution of the chemical activity is studied. The analysis of Fig. 5 enables a parallel to be drawn between the evolution of this chemical activity and the capillary radii. After $\alpha = 8\%$, the capillary spaces between C-S-H hydrate clusters become deactivated: more and more parts of the capillary network are segmented but, at this point, there is no global segmentation of the capillary network. Thus, the formation of outer products slows and we can observe a decrease of chemical activity.

It is now clear that the activity of the hydration sequences depends on the evolution of the capillary network between solid particles. This effect is clearly observed in our specimen that has an important initial granular compactness. Indeed, it is generally admitted that the decrease of the dissipated power is due to the increase of hydrate layer thickness around the anhydrous cement, which prevents the water diffusion into the cement particles. In the case of RPC, the degree of hydration at the maximum of the thermal activity is too low (8%) to provoke the formation of this large hydrate layer.

In order to confirm the evolution of the active capillary radius as a function of hydration degree, electrical conductivity measurements were performed and the results are presented in Fig. 6. The evolution of this conductivity depends both on the ionic concentration and the tortuosity of the medium. Up to $\alpha = 8\%$, the decrease of electrical conductivity is due to the rapid nucleation of the C-S-H hydrates: this nucleation induces the decrease in water

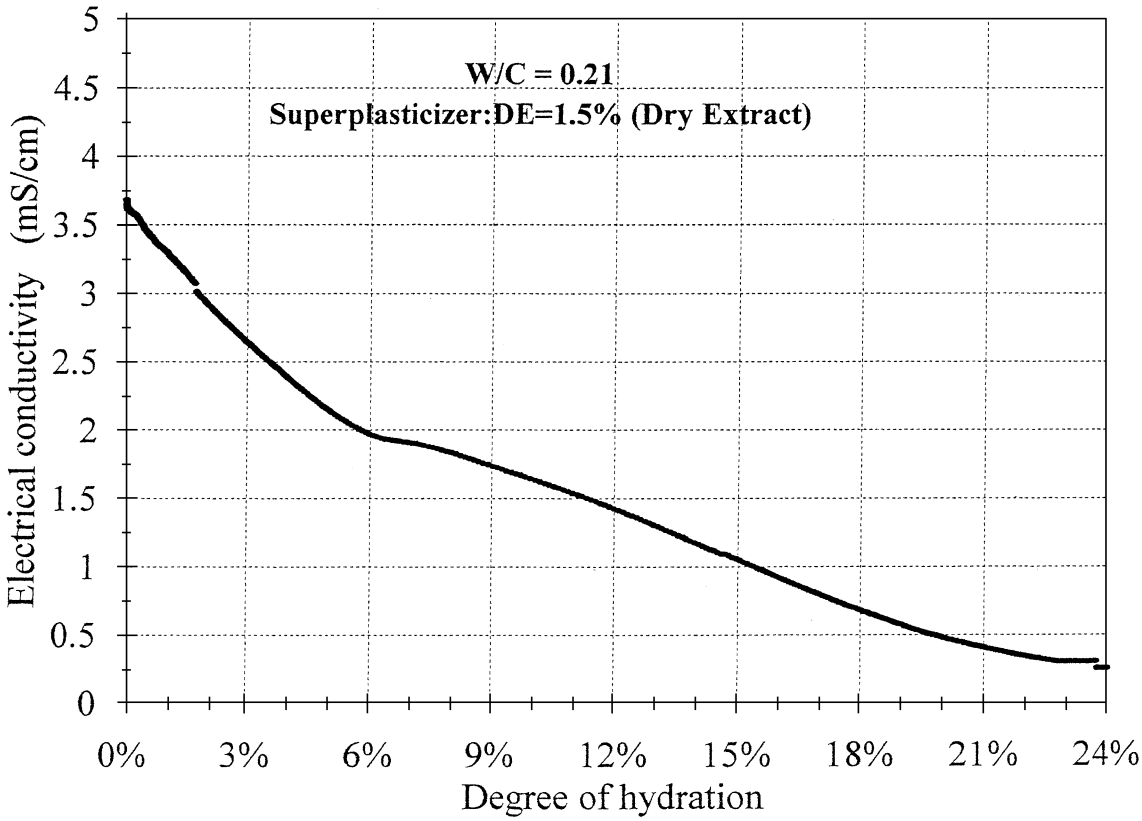

Fig. 6. Electrical conductivity as a function of the degree of hydration.

saturation of the capillary pores by the self-desiccation process and these hydrate formations progressively fill the free spaces between solid particles. However, up to $\alpha = 8\%$, the capillary network keeps its integrity and is not segmented; that explains the fact that the electrical conductivity does not follow exactly the curve of the active capillary radius. After $\alpha = 8\%$, parts of the global capillary network become segmented: the electrical conductivity depends now on the evolution of the internal C-S-H structure and then of the tortuosity of the hydrates matrix. This increase of the tortuosity leads to the lengthening of the ionic transfer. After the maximum of the dissipated power, we observed a division by approximately 5 of the electrical conductivity (from 1.8 to 0.3 mS/cm) and of the active capillary radius (10 to 2 nm). So, a close relationship is observed between the evolution of the capillary radius as given by our model and the electrical conductivity after the maximum of the dissipated power.

4. Conclusion

The use of ultrasonic and autogenous shrinkage measurements allows for the calculation of the active capillary radius of RPCs from the time of mixing when the paste is still liquid. This nonintrusive and online method is consistent with mercury intrusion and desorption test and indicates the existence of two characteristic porous modes. The first one is assimilated to the porous space between the C-S-H hydrates, with typical size ranging from 10 to 20 nm. The second porous mode size ranging between 1 and 2 nm represents the internal porosity of the hydrates. With this original method, the evaluation of the activation of these different porous modes during hydration processes can be performed. As a result, a parallel between the chemical activity and the evolution of the capillary pore radius can be drawn up. Indeed, when the active capillary pore size changes from the first porous mode, the formation of outer products (external C-S-H) decreases because some parts of the capillary network begin to be segmented. This segmentation of the capillary network induces a decrease in the chemical activity because, after this point, the active capillary network is concentrated inside the C-S-H hydrates. At this stage, the consumption of water inside these hydrates allows the formation of inner products, which may reach the bulk of anhydrous cement particles.

This study of the capillary network is crucial because it provides information about the porosity evolution, which is an important parameter in the transport properties of the concrete which are related to its durability. This study must be completed by the comparison of different available methods of porosity evaluation like proton-NMR [12] in order to obtain a better understanding of the porosity evolution in different formulations, such as those with different water contents or granulometry and with various concentrations of additives like superplasticizers.

Acknowledgements

The authors would like to thank Christian Vernet and Fabienne Begaud from the Bouygues Company for their active and efficient participation in this work and particularly for the electrical conductivity measurements.

References

[1] P. Richard, M. Cheyrezy, Composition of reactive powder concretes, Cem. Concr. Res. 25 (7) (1995) 1501–1511.
[2] F. Levassort, F. Cohen Tenoudji, Rapport de D.E.A. d'Acoustique Physique vol. 7, Université Paris VII, Paris, 1991.
[3] A. Boumiz, Etude comparée des évolutions mécaniques et chimiques des pâtes de ciment et mortiers à très jeune âge, Thèse de Doctorat, Université Paris VII, 1995.
[4] V. Morin, F. Cohen Tenoudji, C. Vernet, A. Feylessoufi, P. Richard, Ultrasonic spectroscopic investigation of the structural and mechanical evolutions of a reactive powder concrete, Proc. Int. Symp. on High Performance Concrete and Reactive Powder Concrete, vol. 3, Sherbrooke University, Sherbrooke, 1998, pp. 119–126.
[5] V. Morin, F. Cohen Tenoudji, C. Vernet, Study of the viscoelastic behavior of cement pastes at early ages with ultrasonic waves in echographic mode, 2nd Int. RILEM Workshop on Hydration and Setting, Dijon, 11–13 June, 1997, pp. 317–327.
[6] A. Feylessoufi, F. Cohen Tenoudji, V. Morin, Early ages shrinkage mechanisms of an ultra-high-performance cement-based materials, Cem. Concr. Res. 31 (2001) 1573–1579.
[7] V. Morin, F. Cohen Tenoudji, A. Feylessoufi, Superplasticizer effects on setting and structuration mechanisms of ultrahigh-performance concrete, Cem. Concr. Res. 31 (2001) 63–71.
[8] J. Baron, Les retraits de la pâte de ciment, in: J. Baron, R. Sauterey (Eds.), Le béton hydraulique: connaissance et pratique, Presses de l'Ecole Nationale des Ponts et Chaussés, Paris, 1982, pp. 485–501.
[9] C. Hua, P. Acker, A. Ehrlacher, Retrait d'autodessiccation du ciment: Analyse et modélisation macroscopique, Bull. Liaison. Lab. Ponts Chaussees 196 (1995) 79–89.
[10] H.M. Jennings, A model for the microstructure of calcium hydrate in cement paste, Cem. Concr. Res. 30 (1) (2000) 101–116.
[11] V. Baroghel-Bouny, Caractérisation des pâtes de ciment et des bétons, Méthodes, Analyses, Interprétation, Laboratoire Central des Ponts et Chaussés, LCPC, Paris, 1994, pp. 247–292.
[12] S. Philippot, J.P. Korb, D. Petit, H. Zanni, Analysis of microporosity and setting of reactive powder concrete by proton nuclear relaxation, Magn. Reson. Imaging 16 (5/6) (1998) 515–519.